Papers submitted to the Conference "Applications of Physics in Mechanical and Material Engineering"

Modelling of Phase Transformations in Solid State and Dilatometric Curves Using Interpolation Methods to Determine CCT Diagrams

M. Kubiak[a,*], W. Piekarska[b], T. Domański[a] and Z. Saternus[a]

[a] *Department of Mechanical Engineering and Computer Science, Czestochowa University of Technology, Dąbrowskiego 73, 42-201 Częstochowa, Poland*
[b] *Faculty of Architecture, Civil Engineering and Applied Arts, University of Technology, Rolna 43, 40-555 Katowice, Poland*

Doi: 10.12693/APhysPolA.142.184 *e-mail: marcin.kubiak@pcz.pl

This paper presents mathematical models for the determination of the kinetics of phase transformations in a solid state, volumetric fractions of structural constituents, as well as thermal and structural strain occurring during the cooling process of elements made of carbon steel. The kinetics of phase transformations in a solid state is determined using Johnson–Mehl–Avrami equations for diffusive transformations like ferrite, pearlite, and bainite, and Koistinen–Marburger for martensite transformation. The continuous cooling transformation diagram is determined using interpolation functions and experimental research. Experimental dilatometric analysis for chosen cooling rates is performed in order to define the start and final temperatures as well as start and final times of phase transformations. The increase model for thermal and structural strain is used for the cooling process. Methods of model tuning are used to define thermal expansion coefficients varying in temperature for each analysed phase.

topics: phase transformations, Johnson–Mehl–Avrami (JMA) model, Koistinen–Marburger (KM) model, continuous cooling transformation (CCT) diagram

1. Introduction

Knowledge about thermal phenomena and phase transformations in the solid state accompanying thermal processes is helpful in estimating many technological parameters that should be correctly set to ensure process stability and the best possible quality of steel products [1, 2]. The type of structure and the resulting properties of the heat affected zone (HAZ) depend on the chemical composition of the steel and the thermal cycle parameters such as heating rate, maximum heating temperature, residence time above the A_{c3} temperature, and cooling rate. Changes in the HAZ microstructure, including phase transformations and grain growth, are the cause of significant changes in the properties of this area compared to the base material. Different heating and cooling conditions during heat treatment contribute to the appearance of various structures in HAZ, leading to the different mechanical properties [3–5].

Moreover, during the heating and cooling of steel, temperature field and phase transformations in the solid state are the cause of isotropic strain, which generates residual stress in many technological processes, such as hardening or welding [3, 6]. This is why the determination of the kinetics of phase transformations for the analyzed steel is important in numerical modelling, because reliable determination of the kinetics allows for forecasting the structure composition in the heat treated material. Knowledge of structural heterogeneity is important during the construction design.

In the case of phase transformations in the solid state accompanying the welding processes of steel using moveable heat sources, the variable instantaneous cooling rate in the temperature range 800–500°C or the cooling time in this range is taken into account as a parameter characterizing the steel cooling conditions [2]. The analysis of the phase transformations in the solid state in HAZ of the welded joint is carried out on the basis of the decay diagram of supercooled austenite (welding CCT diagrams). The direct "in situ" method or the simulation dilatometric method are most often used to investigate the kinetics of phase changes under the conditions of welding thermal cycles.

The presented model use the intersection of the cooling curves with the interpolated welding continuous cooling transformation (CCT) diagram to define the start and final times as well as the start and final temperatures. The kinetics of phase transformations in the solid state is modeled using classical Johnson–Mehl–Avrami (JMA) model and Koistinen–Marburger (KM) model [7–9]. A number

TABLE I

Interpolated functions determining the CCT diagram.

Curve (Fig. 2)	Time	Equation	Coefficients
1 F_s	1.98–1000	$y = A_{F_s} + \frac{B_{F_s}}{t}$	$A_{F_s} = 764.38$ $B_{Fs} = -473.38$
2 P_s	2.90–1000	$y = A_{P_s}\ \frac{B_{P_s}}{t}\ t^{C_{P_s}}$	$A_{P_s} = 625.49$ $B_{P_s} = 0.56$ $C_{P_s} = 0.02$
3 B_s	0.69–46	$y = \frac{A_{B_s}\ B_{B_s} + C_{B_s}\ t^{D_{B_s}}}{B_{B_s} + t^{D_{B_s}}}$	$A_{B_s} = -745.97$ $B_{B_s} = 0.0034$ $C_{B_s} = 523.30$ $D_{B_s} = 8.92$
4 $P_f + B_f$	29.10–1000	$y = A_{P_f+B_f} + B_{P_f+B_f}\ t + \frac{1}{2} C_{P_f+B_f}\ t$	$A_{P_f+B_f} = 600.22$ $B_{P_f+B_f} = 0.03$ $C_{P_f+B_f} = -161246.52$
5 M_s	0.10–29.10	$y = A_{M_s} + B_{M_s}\ t$	$A_{M_s} = 409$ $B_{M_s} = 0$
6 M_f	0.10–14.50	$y = \frac{A_{M_s}\ B_{M_s} + C_{M_s}\ t^{D_{M_s}}}{B_{M_s} + t^{D_{M_s}}}$	$A_{M_f} = 219.43$ $B_{M_f} = 32.36$ $C_{M_f} = 484.25$ $D_{M_f} = 1.64$

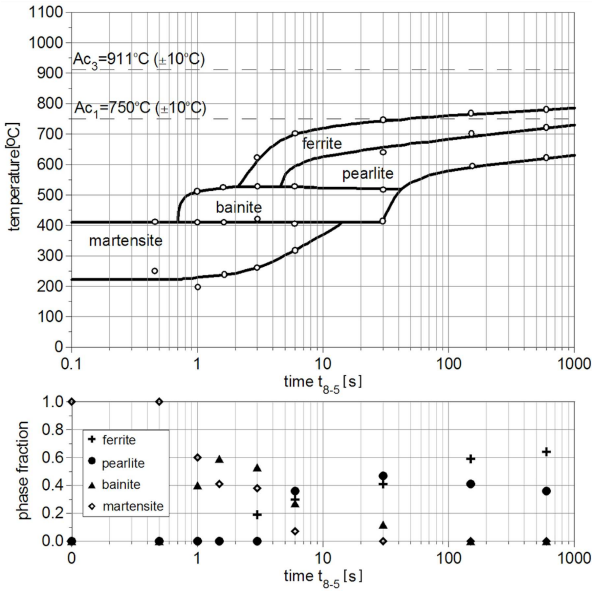

Fig. 1. Experimentally obtained CCT diagram with volume fractions of microstructure constituents.

of simulations of dilatometric curves with different thermal expansion coefficients and structural strain were performed. The so-called "model tuning" considering iterative convergence of the simulation result with the experimental curve is used in order to determine the proper isotropic strain properties for different phases.

2. Definition of interpolated CCT diagram

Start (F_s, P_s, B_s, M_s) and final temperatures (F_f, P_f, B_f, M_f) of each phase transformation and the final fractions of structure constituents during cooling are determined experimentally for S355 steel for a chosen cooling rates (Fig. 1) determined in temperature range 800–500°C. On the basis of the obtained results, interpolation functions are determined to define the CCT diagram (Fig. 2). The interpolation functions used in the calculations are summarized in Table I.

3. Model of kinetics of phase transformations

Numerical estimation of the kinetics of phase transformations in the solid state as well as the microstructure composition were performed for the heating process using constant temperatures A_{c1} and A_{c3} and for cooling on the basis of classic mathematical models [8, 9].

The volumetric fractions of diffusive phases (austenite, ferrite, pearlite and bainite) are determined for the heating and cooling processes, respectively, using JMA formulae

$$\tilde{\eta}_A(T,t) = \eta_{b_{(.)}}\Big(1 - \exp\left(-b\,t^n\right)\Big), \tag{1}$$

$$\begin{aligned} &\eta_{(.)}\left(T,t\right) = \eta^{\%}_{(.)}\,\tilde{\eta}_A\Big(1 - \exp\left(-b\left(t(T)\right)^n\right)\Big),\\ &\underline{\eta}_A - \sum_{k=1}^{4}\eta_k \geq 0, \quad \sum_{k=1}^{5}\eta^{\%}_k = 1, \end{aligned} \tag{2}$$

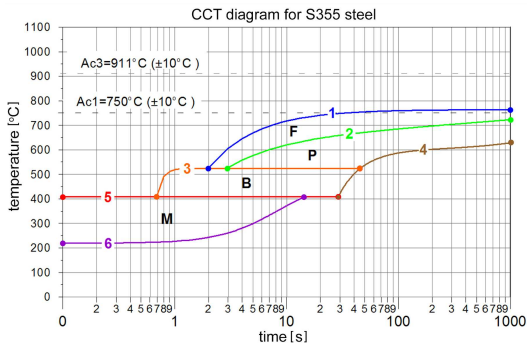

Fig. 2. Interpolated CCT diagram for S355 steel.

where $\eta_{b_{(.)}}$ is a sum of volumetric fractions of the base material structure ($\eta_{b_{(.)}} = 1$), $\eta^{\%}_{(.)}$ is the maximal phase fraction for the determined cooling rate, estimated on the basis of CCT diagram, η_A is the austenite fraction formed due to heating, while η_k is the phase fraction formed before the calculated phase transformation during cooling.

The coefficients b and n are determined by the starting ($\eta_s = 0.01$) and final ($\eta_f = 0.99$) conditions for the phase transformation as follows

$$b(T) = -\frac{\ln(\eta_f)}{(t_s)^{n(T)}} \quad \text{and} \quad n\,(T) = \frac{\ln\left(\frac{\ln(\eta_f)}{\ln(\eta_s)}\right)}{\ln\left(t_s/t_f\right)}, \tag{3}$$

where t is time; $t_s = t_s(T_{sA})$ and $t_f = t_f(T_{fA})$ are the phase transformation start and final times, respectively; T_{sA} and T_{fA} are the start and final temperatures, respectively.

The martensite volumetric fraction (η_M) during cooling is estimated using the KM equation as

$$\eta_M\,(T) = \eta^{\%}_{(.)}\,\tilde{\eta}_A\Big(1 - \exp\left(-k\,(M_s - T)^m\right)\Big), \tag{4}$$

for $T \in [M_s, M_f]$. The coefficient k depends on the martensite phase start and final temperatures (M_s and M_f) also determined using interpolated CCT diagram

$$k = -\frac{\ln(\eta_S)}{M_s - M_f} = -\frac{\ln(0.01)}{M_s - M_f}. \tag{5}$$

4. Model of isotropic strain

Thermal and structural strain during heating and cooling of welded steel is calculated as the solution of the increase of isotropic strain [5]

$$\mathrm{d}\varepsilon^{Tph} = \sum_{i=1}^{i=5}\Big(\alpha_i\eta_i\,\mathrm{d}T - \mathrm{sgn}\,(\mathrm{d}T)\,\varepsilon_i^{ph}\,\mathrm{d}\eta_i\Big), \tag{6}$$

where $\alpha_A = \alpha_A(T)$ are thermal expansion coefficients of austenite, bainite, ferrite, martensite and pearlite, $\varepsilon_i^{Ph} = \varepsilon_i^{Ph}(T)$ is an isotropic structural strain resulting from the transformation of the base material into austenite during heating and each phase (ferrite, pearlite, bainite or martensite) arising from austenite during cooling, $\mathrm{d}\eta_i$ is a volumetric fractions of phases, sgn(.) is a sign function.

5. Results of calculations — tuning of the model

The calculations are made for a constant heating rate $v_h = 100$ K/s and three different cooling rates $v_{8/5} = 2$, 50 and 200 K/s. The same parameters are used in experimental research made on a thermal cycle simulator equipped with thermocouples and a dilatometer. The comparison of calculations with the experiment allowed the proper definition of the thermal expansion coefficients and structural strains. Figures 3–5 presents the calculated kinetics of phase transformations in the solid state and isotropic strain for different cooling rates.

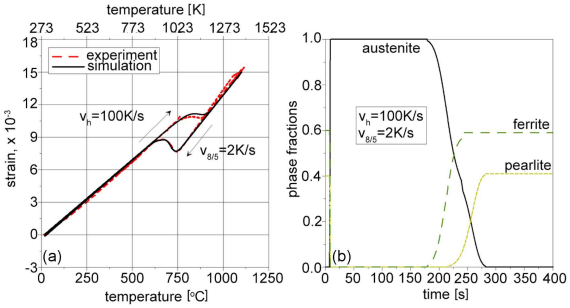

Fig. 3. Calculated (a) isotropic strain and (b) corresponding kinetics of phase transformations. Cooling rate $v_{8/5} = 2$ K/s.

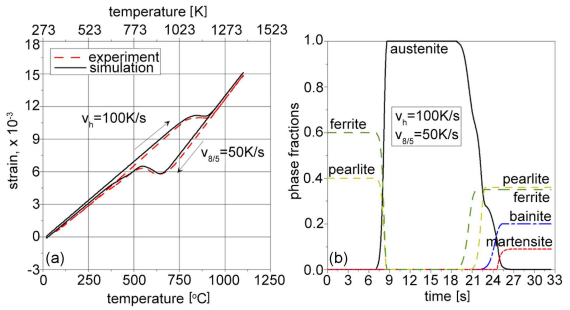

Fig. 4. Calculated (a) isotropic strain and (b) corresponding kinetics of phase transformations. Cooling rate $v_{8/5} = 50$ K/s.

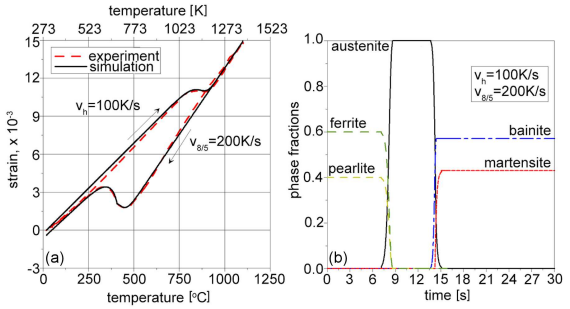

Fig. 5. Calculated (a) isotropic strain and (b) corresponding kinetics of phase transformations. Cooling rate $v_{8/5} = 200$ K/s.

TABLE II

Thermal expansion coefficients and structural strains of microconstituents.

Structural constituent	Thermal expansion coeff. $\alpha_{(i)}$ [1/°C] ($\times 10^{-6}$)		Structural strains $\varepsilon_{(i)}$ ($\times 10^{-3}$)	
austenite	α_A	21.0	ε_A	3.5
ferrite	α_F	14.7	ε_F	3.0
pearlite	α_P	13.7	ε_P	4.0
bainite	α_B	12.5	ε_B	3.5
martensite	α_M	12.0	ε_M	5.7

Table II summarizes the determined coefficients of isotropic strain as a results of model tuning.

6. Conclusions

The use of interpolation functions and the results of experimental research (dilatometric analysis) allowed to describe the CCT diagram (Fig. 2) and to implement the model of phase transformations in the solid state in terms of the kinetics of phase transformations and isotropic strains.

From the comparison of the calculated final fractions of phases during cooling (see Figs. 3b. 4b, 5b), it can be observed that the model agrees well with the experimentally determined final fractions of phases presented in Fig. 1.

The tuning process allowed to define the proper thermal expansion coefficients and proper structural strains for each phase (see Table II).

The developed model can be successfully used in modeling structural phenomena and mechanical phenomena in thermal processes of steel like welding or heat treatment.

References

[1] J.A. Goldak, *Computational Welding Mechanics*, Springer NY, 2005.

[2] W. Piekarska, Analiza numeryczna zjawisk termomechanicznych procesu spawania laserowego: pole temperatury, przemiany fazowe i naprężenia, Wydawnictwo Politechniki Częstochowskiej, Częstochowa 2007.

[3] K.R. Krishma Murthy, F. Akyel, U. Reisgen, S. Olschok, *J. Adv. Join. Process.* **5**, 100080 (2022).

[4] A. Bokota, T. Domański, *Arch. Metall. Mater.* **52**, 277 (2007).

[5] W. Piekarska, M. Kubiak, A. Bokota, *Arch. Metall. Mater.* **56**, 409 (2011).

[6] W. Piekarska, M. Kubiak, Z. Saternus, *Arch. Metall. Mater.* **58**, 1391 (2013).

[7] S. Serajzadeh, *J. Mater. Process. Technol.* **146**, 311 (2004).

[8] J.W. Elmer, T.A. Palmer, W. Zhang, B. Wood, T. DebRoy, *Acta Mater.* **51**, 3333 (2003).

[9] S.-J. Lee, Y.K. Lee, *Scr. Mater.* **60**, 1016 (2009).